High Energy Phenomena in Relativistic Outflows V
AAA Workshop Series 8, 2016
L. J. Pellizza and G. E. Romero, Eds.

Review of the latest results from the Pierre Auger Observatory

Hernan Wahlberg [1] for the Pierre Auger Collaboration[2]

[1] *IFLP - Physics Department, Universidad Nacional de La Plata C.C. 67-1900 La Plata, Argentina.*
[2] *Observatorio Pierre Auger, Av. San Martn Norte 304, 5613 Malargüe, Argentina .*
Full author list: http://www.auger.org/archive/authors_2015_09.html

Abstract. The Pierre Auger Observatory, located in the province of Mendoza, Argentina, was built for detecting and studying ultra-high energy cosmic rays. The Observatory was designed as a hybrid detector covering an area of 3000 km^2 and it has been taking data for more than ten years. In this report a selection of the latest results is presented. These include the observation of the flux evolution and suppression at the highest energies, inferred trends on composition with energy, bounds on photons and neutrinos, and arrival direction studies.

1. Introduction

The Pierre Auger Observatory (Aab et al. 2015) is located in the Province of Mendoza, Argentina. The design of the instrument is based on a hybrid system, a combination of a large surface-detector array (SD) and a fluorescence detector (FD), used to study cosmic rays with energies in excess of 10^{17} eV. The surface detector array, covering an area of over 3000 km^2, comprises 1660 stations, which are arranged on a triangular grid with 1500 m spacing. It samples the electromagnetic and muonic components of extensive air showers (EAS) at a given observation level, with a duty cycle of nearly 100%. The fluorescence detector consists of 27 optical telescopes overlooking the array. On clear moonless nights, these are used to observe the longitudinal development of the shower produced by the primary particle in the atmosphere, by detecting the fluorescence light produced by charged particles along the shower trajectory. The duty cycle of the FD is $\sim$ 13%. Extensions over the base design and future upgrades are summarised in Ghia (2015). The properties of ultra-high energy cosmic rays are studied through the EAS they produce in the atmosphere. These are detected by the complementary surface and fluorescence detectors. In this report a selection of the latest results obtained by the Observatory from data collected since 2004 is presented. Data from a total of 188 000 showers were collected, with a total exposure exceeding 50 000 km^2 sr yr, on a a wide range of sky coverage.

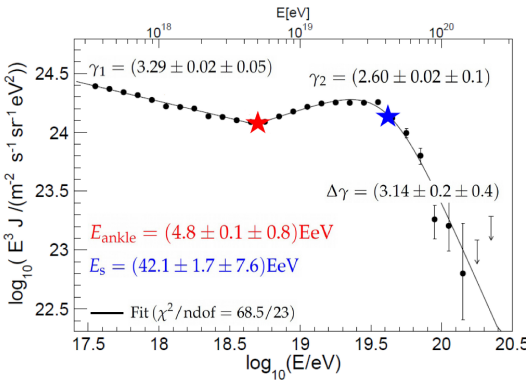

Figure 1. The combined energy spectrum of cosmic rays as measured by the Auger Observatory, fitted with a flux model (reproduced from Valiño 2015). Only statistical uncertainties are shown. The systematic uncertainty on the energy scale is 14%. The number of events is given above the points, which are positioned at the mean value of $\log_{10}$(E/eV). Stars mark the positon of E_{ankle} and E_s as described in the text. The upper limits correspond to the 84% C.L.

2. Analysis and Main Results

2.1. Energy spectrum

The FD allows the measurement of the electromagnetic energy released by the shower in the atmosphere as a function of the atmospheric depth (X). The total primary energy is then derived by integrating this longitudinal profile dE/dX over the X-range and adding an estimate of the so-called invisible energy carried into the ground by high-energy muons and neutrinos. The hybrid measurement is based on the selection and reconstruction of showers observed by the FD in coincidence with at least one SD station, which enables an accurate determination of the shower geometry and consequently of the energy of the primary particle.

The characteristic features of the energy spectrum (Valiño 2015), shown in Figure 1, have been quantified by fitting a model that describes the spectrum by a power law below the ankle $J(E) = J_0(E/E_{ankle})^{-\gamma_1}$ and a power law with a smooth suppression at the highest energies $J(E) \propto (E/E_{ankle})^{-\gamma_2}[1 + (E/E_s)^{\Delta\gamma}]^{-1}$. The results show a spectral index of 2.6 above 4.8×10^{18} eV and a clear steepening of the cosmic-ray flux above an energy around 4.2×10^{19} eV. The dominant systematic uncertainty of the spectrum comes from the overall uncertainty in the energy scale of 14%.

2.2. Mass composition

In this section three different techniques used in the Pierre Auger Observatory to measure mass sensitive observables are presented.

Depth of shower maximum ($X_{\max}$): The measurement of the longitudinal profile of the energy deposit in the atmosphere is described in detail in Porcelli

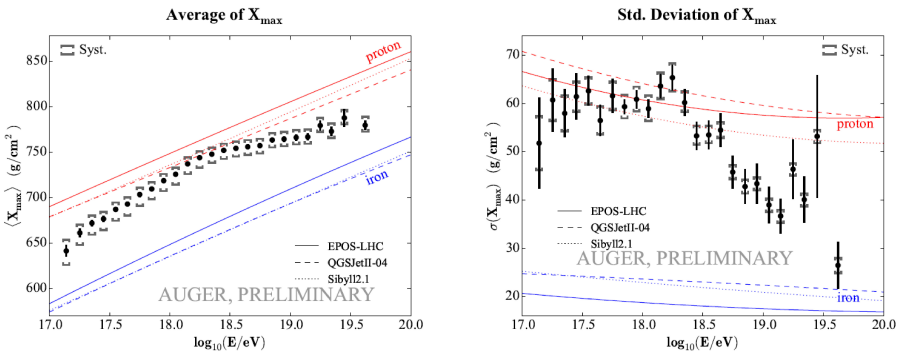

Figure 2. The mean (left) and standard deviation (right) of the measured $X_{\max}$ distributions as a function of energy, compared to air-shower simulations for proton and iron primaries (reproduced from Porcelli 2015).

(2015). In this analysis, hybrid events have been used. The longitudinal profile of the energy deposit is reconstructed from the light recorded by the FD using the fluorescence and Cherenkov yields. The light collected by the telescopes is corrected for the attenuation between the shower and the detector using data from atmospheric monitoring devices. The longitudinal shower profile is finally reconstructed as a function of the atmospheric depth, and $X_{\max}$ is obtained by fitting the profile with a Gaisser-Hillas function. The results for $\langle X_{\max} \rangle$ and its fluctuations $\sigma(X_{\max})$ are shown in Figure 2. Between $10^{17.0}$ and $10^{18.3}$eV, $\langle X_{\max} \rangle$ increases by around 85 g/cm^2 per decade of energy (Figure 2, left). This value, being larger than the one expected for a constant mass composition ($\sim$ 60 g/cm^2/decade), indicates that the mean primary mass is getting lighter. Around $10^{18.3}$ eV the observed rate of change of $\langle X_{\max} \rangle$ becomes significantly smaller ($\sim$ 26 g/cm^2/decade) indicating that the composition is becoming heavier. The fluctuations start to decrease at around the same energy $\sim 10^{18.3}$ eV as shown in Figure 2 (right).

Muon Production Depth (MPD): The time of the signals recorded by the SD can be used to obtain information about the longitudinal development of the hadronic component of extensive air showers in an indirect way. It is shown in Collica (2015) that it is possible to reconstruct the MPD, i.e., the distance to the production of the muon measured parallel to the shower axis, by converting the time distribution of the signal recorded by the SD stations into muon production distances using an approximate relation between production distance, transverse distance and time delay. From the MPDs, an observable can be defined, $X^{\mu}_{\max}$, as the depth along the shower axis where the number of produced muons reaches a maximum. Figure 3 shows the variations of $\langle \ln A \rangle$ with energy that is extracted from a comparison with each of two hadronic interaction models tuned with the latest LHC data.

Signal Time Asymmetry: It is well known that the first portion of the signal in each SD detector is dominated by the muon component which arrives earlier and over a period of time shorter than the electromagnetic (photons and electrons)

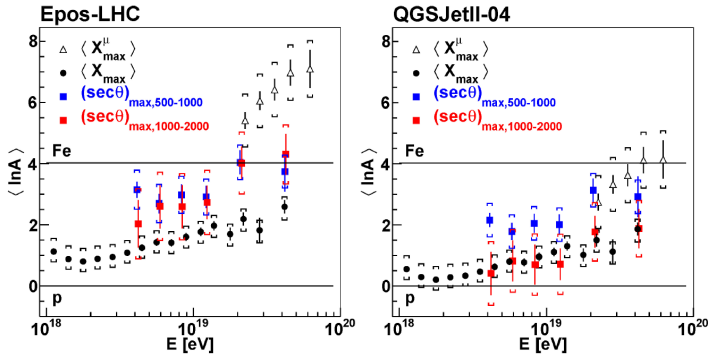

Figure 3. $\langle \ln A \rangle$ vs E as predicted by Epos-LHC and QGSJetII-04. Results from the time asymmetry method in both r-intervals are compared with those from the elongation curve and the MPD method (reproduced from Minaya 2015).

particles (EM). This is because muons travel in almost straight lines whereas the electromagnetic particles suffer multiple scattering. Due to the absorption of the EM component, the number of these particles at ground level depends, for a given energy, on the distance to the shower maximum and therefore on the primary mass. In consequence, the time profile of particles reaching the ground is sensitive to the cascade development as the higher the production height, the narrower the time pulse. Equivalently, for inclined showers, both the magnitude and risetime of the signals depend on the azimuth since particles reaching late detectors traverse longer atmospheric paths than those arriving at early detectors. The method uses the above mentioned azimuthal asymmetry to describe the shower profile (Minaya 2015) and has been carried out independently for two intervals from the shower core, i.e., 500-1000m and 1000-2000m.

Figure 3 shows the variations of $\langle \ln A \rangle$ with energy summarising the results from the measurements of $X_{\max}$, MPD and asymmetry. The values of $\langle \ln A \rangle$ derived from the Epos-LHC model are consistent for the two distance ranges for the asymmetry. However this is not the case for QGSJetII-04 as can be seen in the figure. In an overall comparison neither model provides an accurate description when taking into account the different shower parameters.

2.3. Search for photons and neutrinos

Limits to the flux of neutrinos: Neutrinos, unlike protons and heavier nuclei, can generate showers initiated deep into the atmosphere. The main signature of these deep showers in the SD is a significant electromagnetic component spread in time over hundreds of nanoseconds, especially in the region on the ground at which the shower arrives earlier. On the other hand, hadron-induced showers start high in the atmosphere, and for very inclined showers their electromagnetic component is fully absorbed and only high energy muons and their radiative and decay products reach the surface, concentrated within a few tens of nanoseconds. The criteria for selecting showers initiated by neutrinos can be found in Bleve (2015) and references therein. Figure 4 (left) shows upper

limits to the diffuse flux of UHE neutrinos at 90% C.L. in integrated and differential forms. These limits are compared with cosmogenic neutrino models, the Waxman-Bahcall bound, and limits from IceCube and ANITA. All neutrino limits and fluxes are converted to single flavour. As can be seen in the figure, cosmogenic models assuming a pure primary proton composition at the sources with strong evolution (FRII-type) of the sources and constrained by the GeV observations of Fermi-LAT are disfavoured. The current Auger limit is approaching the fluxes predicted under a range of assumptions for the composition of the primary flux, source evolution, and model for the transition from galactic to extragalactic cosmic rays. A 10-fold increase in the exposure will be needed to reach the most optimistic predictions in the case of a pure iron composition at sources, out of the range of the current configuration of the Observatory.

Limits to the photon flux: Showers induced by photons are characterised by a lower content of muons and larger average depth of maximum longitudinal development than showers initiated by nuclei with the same energy. This is due to the radiation length being more than two orders of magnitude smaller than the mean free path for photo-nuclear interactions, causing a reduced transfer of energy to the hadron/muon channel, and to the development of the shower being delayed by the typically small multiplicity of electromagnetic interactions. At large distances from the axis, photon showers produce typically smaller signals than expected from the lateral distribution of nuclear showers. This feature, together with the risetime of the signal in the station, are suitable variables for the search for photons (Bleve 2015). The limits to the integral flux are shown in Figure 4 (right) . The figure also shows results from Telescope Array (TA), Yakutsk (Y), Haverah Park (HP), AGASA (A) and predictions from several top-down and cosmogenic photon models. The limits to the diffuse flux of photons obtained with the Auger Observatory are the most stringent for E $>$ 10 EeV and start to constrain the most optimistic predictions of cosmogenic photon fluxes under the assumption of a pure proton composition at the sources.

2.4. Arrival directions

Intrinsic and large angular scale anisotropy studies: The search for intrinsic anisotropies in the distribution of arrival directions of cosmic rays with energies above 40 EeV is performed by computing the angular auto-correlation function, and by looking at potential excesses in circular windows across the exposed sky. Both tests gave results that are compatible with isotropic expectations (Aublin 2015). Rayleigh analyses are also performed both in right ascension and in azimuth angle, and the dipole components are obtained along the equatorial plane and along the rotation axis of the Earth. In the energy band E $>$8 EeV a dipole component with amplitude (0.073$\pm$0.015) and pointing in the direction (α;δ)=(95°$\pm$13°,39°$\pm$13°) is found, above isotropic expectations (Samarai 2015).

Search for cross-correlations with astrophysical sources: For the cross-correlation with astrophysical sources, a scan is done over events energies from 40 EeV up to 80 EeV and in angular scale, between 1 and 30 degrees. For sources in the catalogs, a maximum distance cut D is imposed, that can vary from 10 Mpc up to 200 Mpc. For each value of D, the fraction of isotropic simulations having an equal or higher number of pairs than the data is computed, and a search for its

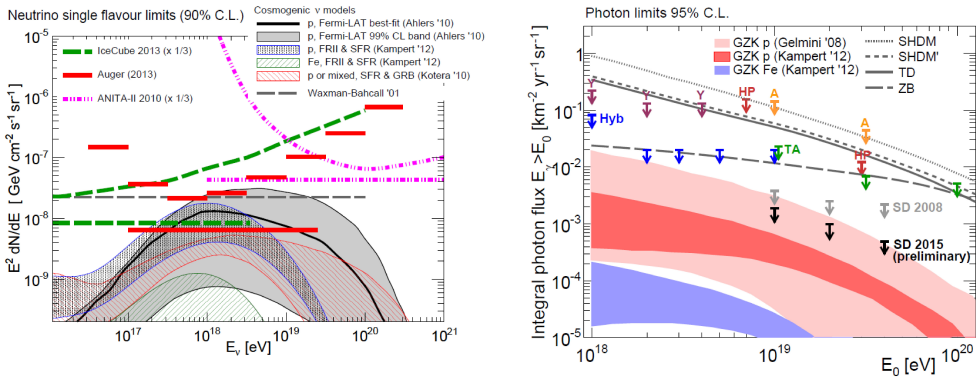

Figure 4. Left: upper limits to the diffuse flux of UHE neutrinos at 90% C.L. in integrated (horizontal lines) and differential forms. Limits described in this work (red lines) are compared with cosmogenic neutrino models. Right: Upper limits at 95% C.L. to the diffuse flux of UHE photons derived from recent Auger data (black) shown together with previous results from the Pierre Auger Observatory with hybrid (Hyb) and SD data (reproduced from Bleve 2015).

minimum f_{min} is carried out. The associated post-trial probability is determined as the fraction of isotropic realisations that lead to a lower than or equal value of f_{min} under a similar scan. The cross-correlation from three complementary astrophysical catalogues has been performed, namely the 2MRS catalogue of galaxies, the Swift-BAT X-ray catalogue of AGNs, and a catalogue of radio galaxies with jets, together with a specific analysis of the arrival directions around the Cen A radio galaxy. The results are summarised in Aublin (2015). The penalised chance probabilities, accounting for the scan on parameters are of the order of a few percent, reach the 1% level when selecting only the brightest AGNs of the Swift-BAT catalogue or with the Cen A radio galaxy. From the results it could be noted that all minima, despite not being statistically significant, occur for a value of the maximum distance of approximately 80-90 Mpc.

References

Aab A., et al. (The Pierre Auger Collab.) 2015, Nucl. Instrum. Meth. A 798, 172
Aublin J., for the Pierre Auger Collab. 2015, Proc. 34th ICRC, PoS(ICRC2015)310
Bleve C., for The Pierre Auger Collab. 2015, Proc. 34th ICRC, PoS(ICRC2015)1103
Collica L., for The Pierre Auger Collab. 2015, Proc. 34th ICRC, PoS(ICRC2015)336
Ghia P.L., for the Pierre Auger Collab. 2015, Proc. 34th ICRC, PoS(ICRC2015)034
Minaya I.A., for The Pierre Auger Collab. 2015, Proc. 34th ICRC, PoS(ICRC2015)405
Porcelli A., for The Pierre Auger Collab. 2015, Proc. 34th ICRC, PoS(ICRC2015)420
Samarai I.A., for the Pierre Auger Collab. 2015, Proc. 34th ICRC, PoS(ICRC2015)372
Valiño I., for The Pierre Auger Collab. 2015, Proc. 34th ICRC, PoS(ICRC2015)271